Colloid Polym Sci (2007) 285:1175–1180
DOI 10.1007/s00396-007-1685-x

SHORT COMMUNICATION

# Growth of hydroxyapatite nanocrystals on polymer particle surface

**Susann Schachschal · Andrij Pich · Hans-Juergen Adler**

Received: 6 September 2006 / Accepted: 26 April 2007 / Published online: 31 May 2007


**Abstract** In the present paper, we describe the preparation of hybrid particles consisting of polymeric core with deposited hydroxyapatite (HAp) nanocrystals. Polystyrene submicron particles modified by $\beta$-diketone groups have been used as templates for the growth of HAp. Hybrid particles with HAp nanocrystal content between 7 and 50 wt% have been prepared. Microscopy studies indicate that hybrid particles exhibit "raspberry" morphology, and HAp nanoparticles are not homogeneously distributed on the polymer particle surface. The increase in the HAp content on the polymer particle surface reduces the colloidal stability of the hybrid particles because of the vanishing of the surface charge.

**Keywords** Hydroxyapatite · Hybrid particles

## Introduction

The considerable development in the field of material science is inspired by the biological composite materials such as bones, teeth, and shells because of their unusual structural, morphological, and mechanical properties [1, 2]. Such hybrid materials unlike synthetic composites are characterized by the high degree of organization of the inorganic phase. The biological hybrid materials can be formed in vivo as ordered arrays by complicated physico-chemical processes, which are not completely understood until now. Therefore, the biomimetic preparation of composite materials in synthetic systems received recently a strong interest and stimulated intensive research in this field. The hydroxyapatite (HAp, $Ca_{10}(PO_4)_6(OH)_2$) belongs to the most important biominerals, which can be found in natural hard tissues [2]. However, hydroxyapatite as well as other calcium phosphates shows poor mechanical properties (low elasticity and high brittleness). The combination of HAp with polymeric matrix leads to the hybrid materials exhibiting high flexibility, mechanical strength, biocompatibility, and good processing/shaping [3]. The interaction of the HAp with polymeric matrix is realized by covalent bonds, hydrogen bonds [4], dipole–dipole interactions, or complexation of $Ca^{2+}$-ions by functional groups such as amine, acetylamine, or hydroxyl [5]. In this way, the polymeric matrix plays an important role in the nucleation and growth of HAp crystals and determines their size, morphology, and orientation in the composite material. The most important application fields for hybrid materials containing HAp are tissue engineering [6], implants [3], drug delivery systems [7, 8], catalysis [9, 10], adsorbents [11], and protein chromatography [12, 13].

A large variety of polymeric materials have been used as templates for the synthesis of HAp such as protein collagen [14], poly(L-lactic acid) [15], poly(aspargic acid) [16], alginates [17], gelatine [18], chitosan [4, 5, 19], chitin [20], dendrimers [21, 22], hydrogels [23–25], etc. The use of polymeric particles as templates for the growth of HAp nanocrystals has not been intensively studied. Polymeric particles as templates provide several advantages such as uniform size, extremely large surface area, and enormous possibilities for the surface functionalization. In this way, well-defined hybrid particles can be prepared for use in chromatography columns or as catalyst in different technical systems. An applicability of polymeric particles coated by $Pd^0$ for the growth of HAp nanocrystals has been

S. Schachschal · A. Pich (✉) · H.-J. Adler
Institute of Macromolecular Chemistry and Textile Chemistry,
Technische Universität Dresden,
01062 Dresden, Germany
e-mail: apich@chem.utoronto.ca

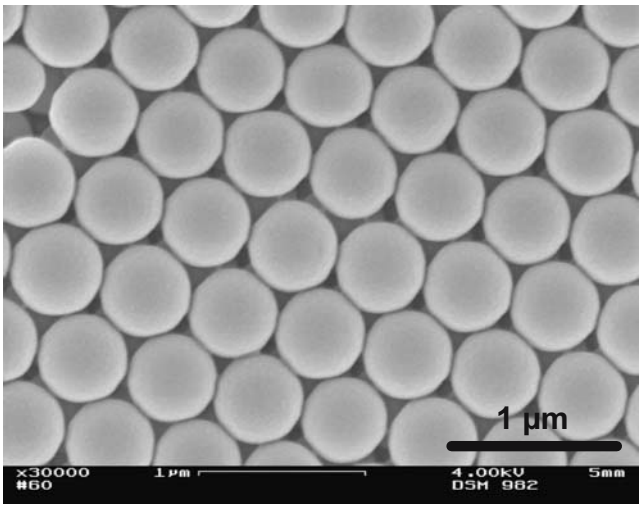


**Fig. 1** SEM image of PS-AAEM particles (hydrodynamic radius $R_h$= 321 nm)

demonstrated by Tamai et al. [26] The homogeneous growth of the hydroxyapatite layer on the particle surface led to the formation of polystyrene core-HAp shell hybrids. Recently, Sukhorukov et al. [27] demonstrated the utilization of the pH-sensitive polyelectrolyte capsules for the growth of hydroxyapatite nanocrystals and fabrication of hybrid hollow spheres. In the present paper, we investigate the growth of the hydroxyapatite nanocrystals on the surface of monodisperse polymeric particles bearing $\beta$-diketone groups. Those particles have been prepared by copolymerizaton of styrene (ST) and acetoacetoxyethyl methacrylate (AAEM) in surfactant-free heterophase polymerization process. In our previous studies, PS-AAEM particles have been successfully used for the controlled growth of the $Fe_2O_3$ [28], ZnO [29], and ZnS [30] nanocrystals on their surface. The aim of the present study was to prepare hybrid colloids coated with hydroxyapatite nanoparticles and to investigate their morphology and colloidal properties. The reason for using PS-AAEM particles as a template originates from the versatile properties of surface-grafted $\beta$-diketone groups able to chelate metals and participate in a wide range of post-modification reactions with amines, aldehydes [31, 32], as well as immobilization of proteins [33]. This gives a possibility to design interesting hybrid materials containing hydroxyapatite suitable for the use in protein separation or catalysis.

## Experimental

### Materials

ST (Fluka) and acetoacetoxyethyl methacrylate (97%; AAEM; Aldrich) were purified by conventional methods and then vacuum distilled under nitrogen. Radical initiator sodium peroxodisulfate (97%; SPDS; Aldrich) was used as commercially available. Distilled water was employed as polymerization medium. Calcium nitrate tetrahydrate [$Ca(NO_3)_2{\cdot}4H_2O$; Grüssing, 99%], diammonium hydrogenphosphate [$(NH_4)_2HPO_4$; Riedel-de Haën, 99%), and ammonia solution (Fisher Chemicals, 25%) have been used as received.

### *Core synthesis*

Preparation of PS-AAEM particles has been performed in the following way. Double-wall glass reactor equipped with stirrer and reflux condenser was purged with nitrogen. Water (170 g) and appropriate amounts of ST (19.5 g) and AAEM (0.5 g; 2.5% of the ST amount) were added into reactor and stirred at room temperature. After 10 min, temperature was increased to 70°C, and an aqueous solution of initiator (0.3 g in 10 g of water) was added to start the polymerization process. Latex was prepared at ca. 10% solid content. The hydrodynamic radius of obtained PS-AAEM particles determined by dynamic light scattering (DLS) was 321 nm.

The emulsifier-free heterophase polymerization leads to the formation of the monodisperse polystyrene particles with grafted hydrophilic AAEM-rich surface layer (see Fig. 1). As it has been demonstrated in our previous studies [26], the variation of the AAEM content in the system gives a possibility to control the particle size in the range 250–800 nm.

**Table 1** Ingredients used for the preparation of hybrid particles

| Sample | PS-AAEM (g) | $Ca(NO_3)_2{\cdot}4\ H_2O$ (g) | $(NH_4)_2HPO_4$ (g) | $HAp^T$ (wt%) | $HAp^M$ (wt%) | pH |
|---|---|---|---|---|---|---|
| 1 | 1.86 | 0.4621 | 0.1547 | 9.56 | 7.44 | 10.2 |
| 2 | 0.93 | 0.4621 | 0.1547 | 17.45 | 16.11 | 10.3 |
| 3 | 0.93 | 0.6932 | 0.2321 | 24.08 | 23.08 | 10.2 |
| 4 | 0.93 | 1.1553 | 0.3868 | 34.58 | 32.84 | 10.2 |
| 5 | 1.39 | 2.757 | 0.923 | 45.76 | 42.92 | 10.1 |
| 6 | 1.39 | 3.453 | 1.156 | 51.38 | 48.43 | 10.2 |

*T* theoretical; *M* measured by TGA

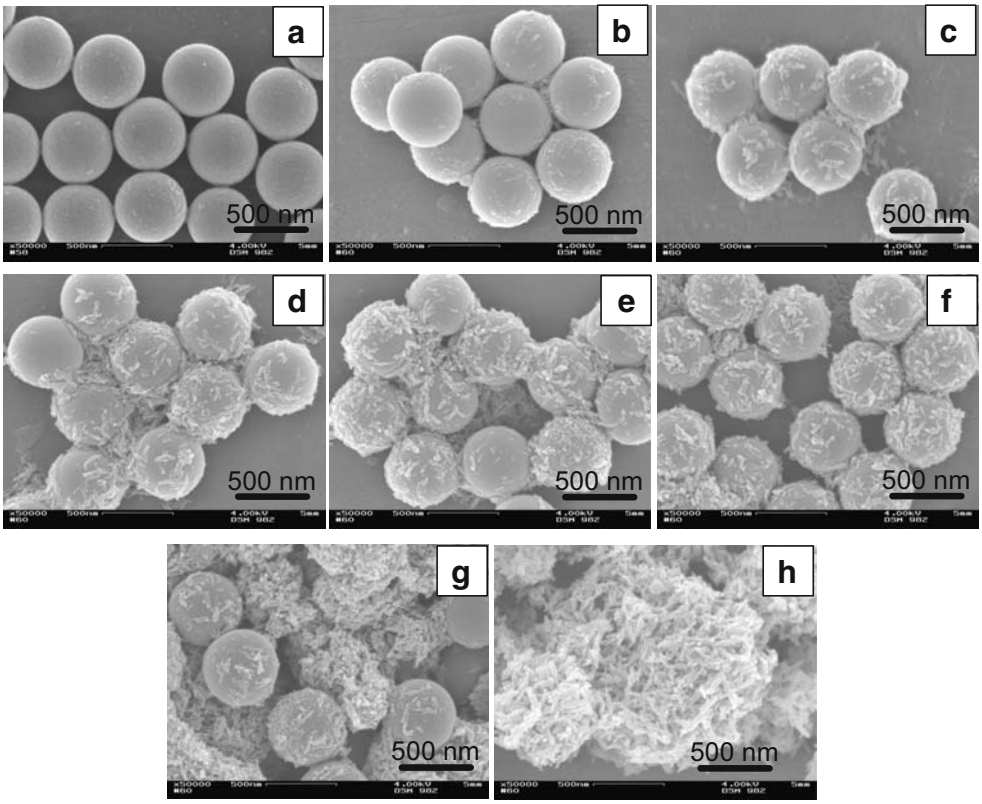


**Fig. 2** SEM images of hybrid particles: **a** PS-AAEM core; **b** 7.44% HAp; **c** 16.11% HAp; **d** 23.08% HAp; **e** 32.84% HAp; **f** 42.92% HAp; **g** 48.43% HAp; **h** HAp

*Deposition of hydroxyapatite*

Appropriate amount of $Ca(NO_3)_2 \cdot 4H_2O$ was dissolved in PS-AAEM latex, and the pH value was adjusted to 10 by addition of 25% $NH_4OH$. In a separate flask, appropriate $(NH_4)_2HPO_4$ amount was dissolved in water, and pH value was adjusted to 10 by addition of 25% $NH_4OH$. The $(NH_4)_2HPO_4$ solution was added under continuous stirring to the polymeric dispersion containing $Ca(NO_3)_2$, and the mixture was stirred for 24 h at 27°C. Table 1 shows the ingredient amounts used in separate runs.

The pH value of the reaction mixture was permanently controlled and kept at 10. Obtained hybrid particles have been cleaned in dialysis bags (Spectra/Por® 3—MWCO 3500).

Analytical techniques

For determination of latex particle size, a commercial laser light scattering (LLS) spectrometer (ALV/DLS/SLS-5000) equipped with an ALV-5000/EPP multiple digital time correlator and laser goniometer system ALV/CGS-8F S/N 025 was used with a helium-neon laser (Uniphase 1145P, output power of 22 mW, and wavelength of 632.8 nm) as the light source.

Zeta-potential measurements have been performed with the Zetasizer3000 (Malvern Instruments). The pH adjustment has been realized by the addition of HCl and NaOH. $10^{-3}$ M KCl solution was used for the preparation of diluted particle solutions.

Stability measurements of latex dispersions were performed with the separation analyzer LUMiFuge 114 (L.U.M. GmbH, Germany). Measurements were made in glass tubes at acceleration velocities from 500 to 3,000 rpm. The slope of sedimentation curves was used to calculate the sedimentation velocity and to get information about the stability of the samples.

Scanning electron microscope (SEM) images were taken with the Gemini microscope (Zeiss, Germany). Samples were prepared in the following manner. Dispersions were diluted with deionized water, dropped onto cleaned support, and dried at room temperature or 45°C. Samples were coated with thin Pd/Au layer to increase the contrast and quality of the images. Pictures were taken at a voltage of 4 kV.

The X-ray diffraction (XRD) measurements have been performed with the Siemens P5005 Powder X-ray diffractometer (source—CuK$\alpha$; $\lambda$=1,54 Å).

Infrared (IR) spectra were recorded with the Mattson Instruments Research Series 1 FTIR spectrometer. Dried polymer samples were mixed with KBr and pressed to form a tablet.

To determine the hydroxyapatite content in composite particles, the thermogravimetrical measurements have been performed with the TGA 7 Perkin Elmer instrument (Pyris-Software Version 3.51). Before the measurement samples

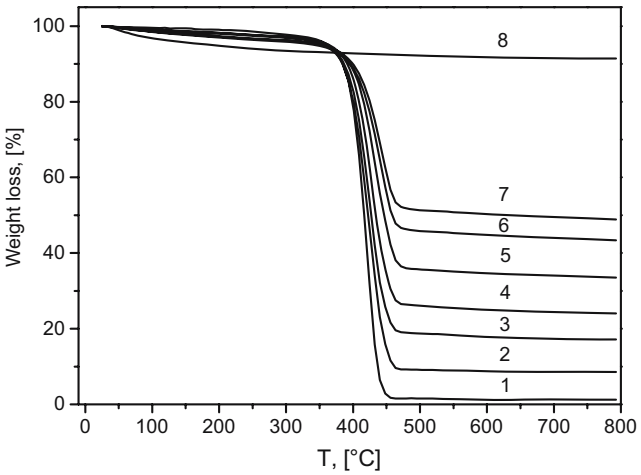


**Fig. 3** TGA curves of investigated samples: *1*, PS-AAEM; *2*, 7.44% HAp; *3*, 16.11% HAp; *4*, 23.08% HAp; *5*, 32.84% HAp; *6*, 42.92% HAp; *7*, 48.43% HAp; and *8*, HAp

were vacuum dried for approximately 48 h, samples were analyzed in temperature range of 25–800°C (heating rate of 10 K/min in nitrogen atmosphere, measurement error±0.5%).

## Results and discussion

The hydroxyapatite formation in the presence of PS-AAEM particles led to the formation of the hybrid particles. Figure 2 shows SEM images of different samples prepared by using different $Ca(NO_3)_2{\cdot}4H_2O$ and $(NH_4)_2HPO_4$ concentrations (see Table 1). This led to the gradual increase in HAp amount in the investigated system.

Figure 2 indicates that as HAp content increases, more inorganic crystals can be observed, which correlates with the TGA data summarized in Table 1. At low HAp contents, the inorganic crystals are localized mostly on the particle surface. However, starting from the sample containing 33% HAp, inorganic crystals can be also found beside polymeric templates. Microscopy images indicate that HAp nanocrystals are not homogeneously distributed on the polymeric particle surface.

These two effects can be caused by the simultaneous crystal formation on the latex particle surface and in the solution. Because of the ability of the $\beta$-diketone groups complex metal ions, we suggest that some fraction of the $Ca^{2+}$ ions will be localized at the PS-AAEM particle surface, leading to the nucleation of HAp nanocrystals. At the same time, free $Ca^{2+}$ ions can lead to the nanocrystals formation in the aqueous phase, which can aggregate and form large agglomerates (see example Fig. 2g) or precipitate on the particle surface. The aggregate formation from single HAp nanocrystals is strongly pronounced at high concentrations of the starting ingredients because of the higher amount of free $Ca^{2+}$ ions and acceleration of the reaction rate. Therefore, the formation of the compact HAp shell on the latex particle surface was not achieved, and hybrids with rather "raspberry" morphology have been obtained.

The thermogravimetrical analysis (TGA) of the composite particles has been performed to determine the HAp content and check the thermal stability of the samples. The experimental TGA curves are summarized in Fig. 3.

The TGA curve of the HAp sample presented in Fig. 3 shows a little weight loss around 100°C probably because of the removal of the residual water. The TGA curve of the PS-AAEM sample exhibits a sharp weight loss step between 400 and 450°C, which corresponds to the thermal degradation of the polystyrene. The TGA curves for composite samples indicate the presence of both HAp and PS-AAEM in the composite material. The rising HAp amount in composite samples can be tracked by the systematic slight increase in the weight loss around 100°C and increase in the residual sample weight at 800°C. The interesting phenomenon can be observed in the temperature range of polymer decomposition. The decomposition step breath becomes broader with an increase in the HAp content in the composite samples, which indicates that inorganic nanocrystals improve to some extent the thermal stability of the polymeric core.

The chemical composition of the HAp has been examined by energy dispersive X-ray spectroscopy. The elemental analysis gives a possibility to determine Ca/P ratio, which is quite an important characteristic of HAp. The EDX results summarized in Table 2 suggest that in all samples, the Ca/P ratio oscillates between 1.6 and 2 (theoretical value for HAp is 1.67). The Ca/P ratio higher

**Table 2** Elementary analysis data of hybrid particles (EDX data)

| Sample | c(HAp) (wt%) | C (at.%) | O (at.%) | Ca (at.%) | P (at.%) | Ca/P |
|---|---|---|---|---|---|---|
| 1 | 7.44 | 81.17 | 16.20 | 1.61 | 1.02 | 1.58 |
| 2 | 16.11 | 75.10 | 19.74 | 3.41 | 1.75 | 1.94 |
| 3 | 23.08 | 91.74 | 4.72 | 2.23 | 1.30 | 1.71 |
| 4 | 32.84 | 82.78 | 13.46 | 2.49 | 1.28 | 1.94 |
| 5 | 42.92 | 74.89 | 20.57 | 2.80 | 1.73 | 1.62 |
| 6 | 48.43 | 74.63 | 20.38 | 3.37 | 1.62 | 2.08 |

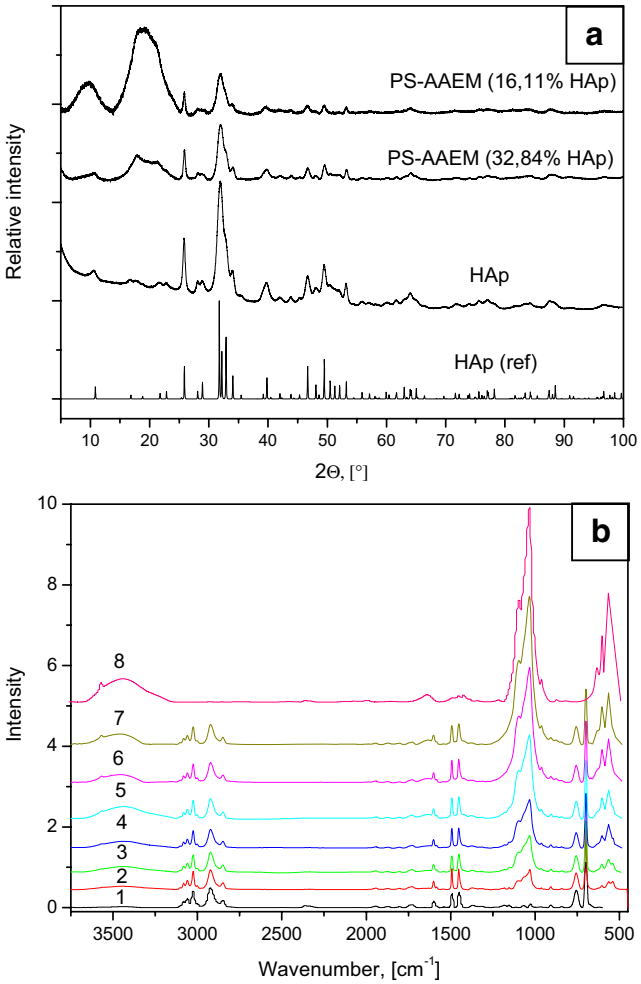


**Fig. 4** XRD patterns of hybrid particles (**a**); IR spectra of hybrid particles: *1*, PS-AAEM; *2*, 7.44%; *3*, 16.11%; *4*, 23.08; *5*, 32.84%; *6*, 42.92%; *7*, 48.43%; and *8*, HAp (**b**)

than the theoretical value indicates that some substitutions of other ions are probably present in the crystal structure instead of phosphate (we assume this to be carbonate initially present in aqueous phase).

The XRD data for selected samples presented in Fig. 4a suggest that hybrid materials exhibit characteristic signals, which correlate with the reference spectra for HAp. The signal intensity is strongly dependent on the HAp amount in the sample. The intensity of broad reflexes at low angles attributable to the polymeric template increases at low HAp contents.

The characteristic signals for the polystyrene units in the IR spectra appear at 1,450, 1,500, and in the region from 2,800 to 3,100 $cm^{-1}$ (Fig. 4b). A weak signal at 1,750 $cm^{-1}$ is related to the carbonyl group of the acrylate units. Those signals can also be found in the hybrid samples. The most important absorption bands of the phosphate group in the HAp structure appear at 565, 603, 1,034, and 1,094 $cm^{-1}$. Figure 4b shows that the increase in the HAp content in the hybrid particles induces the stepwise increase in the band intensity for the inorganic component. The intensity of the broad band in the region from 3,100 to 3,600 $cm^{-1}$ related to the crystal water increases with HAp content.

The colloidal properties of obtained hybrid particles have been investigated by measuring the electrophoretic mobility (later transformed into zeta-potential) and sedimentation velocity. Zeta-potential measurements for selected samples are summarized in Fig. 5a. Strong negative values determined for PS-AAEM particles in the whole pH range can be explained by the hydrolysis of AAEM units and formation of the carboxy groups. The HAp shows weak negative potential in the basic region and approaches zero at pH=7. Hybrid samples show tendency to lower surface charge if the HAp content increases because of the coverage of the particle surface with inorganic nanocrystals. The reduction in the surface charge with the increase in HAp content leads to partial destabilization of colloidal system, and hybrid particles tend to aggregate especially those containing much hydroxyapatite.

The determination of the particle sedimentation velocity confirms this conclusion. Figure 5b indicates that, generally, the sedimentation velocity increases with HAp content. This result is due to the decrease in the surface potential as demonstrated in Fig. 5a that reduces considerably repulsive forces in the system. However, the sedimentation velocity increases dramatically if the HAp content approaches 30%. The reason for such behavior is that HAp crystals or their aggregates appear beside hybrid particles (see Fig. 2e) and cause flock formation. To improve the colloidal stability of

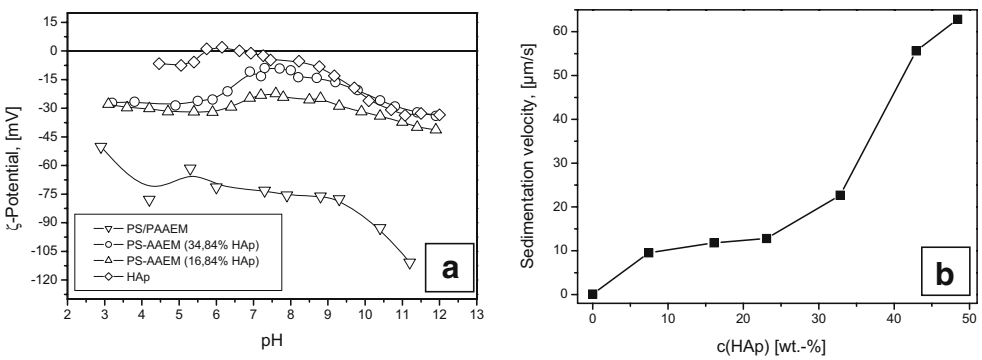


**Fig. 5** Zeta-potential as a function of pH (**a**) and sedimentation velocity as a function of HAp content (determined at 300 rpm;**b**)

the hybrid particles in the present system, it might be advantageous to graft some hydrophilic macromonomers [for example, low molecular weight poly(ethylene oxides)] during the polymer particle synthesis step. This can probably improve the particle stabilization by sterical mechanism after HAp deposition, and additionally, more homogeneous distribution of the HAp nanocrystals on the particles surface can be achieved.

## Conclusions

In the present work, hybrid particles have been prepared by the growth of hydroxyapatite nanocrystals on the surface of polymeric particles. The microscopy results suggest the formation of the "raspberry" morphology, and formation of the compact HAp shell has not been achieved. The HAp content in the hybrid particles can be scaled up to 43 wt% by controlling the reactant concentrations. At higher HAp contents, formation of the secondary HAp crystals have been detected, which tend to form large aggregates. The incorporation of the HAp decreases the surface charge of particles, and therefore, colloidal stability vanishes.

**Acknowledgment** Authors are thankful to Dr. Y. Prots for the XRD measurements and Mrs. E. Kern for the SEM measurements. The financial support from the Deutsche Forschungsgemeinschaft (DFG) is highly acknowledged.

## References

1. Mann S, Webb J, Williams RJP (1989) Biomineralization: chemical and biological perspectives. VCH, New York
2. Dorozhkin SV, Epple M (2002) Angew Chem 114:3260–3277
3. Neumann M, Epple M (2006) Eur J Trauma 2:125–131
4. Li Z, Yubao L, Aiping Y, Xuelin P, Xuejiang W, Xiang Z (2005) J Mater Sci: Mater Med 16:213–219
5. Rusu VM, Ng CH, Wilke M, Tiersch B, Fratzl P, Peter MG (2005) Biomaterials 26:5414–5426
6. Rodríguez-Lorenzo LM, Ferreira JMF (2004) Materials Res Bull 39:83–91
7. Kim H-W, Knowles JC, Kim H-E (2005) J Mater Sci: Mater Med 16:189–195
8. Barroug A, Glimcher MJ (2002) J Orthop Res 20:274–280
9. Zahouily M, Bahlaouan W, Bahlaouan B, Rayadh A, Sebti S (2005) Arkivoc 13:150–161
10. Wakamura M (2005) Fujitsu Sci Tech J 41(2):181–190
11. Kawai T, Ohtsuki C, Kamitakahara M, Tanihara M, Miyazaki T, Sakaguchi Y, Konagaya S (2006) Environ Sci Technol 40:4281–4285
12. Felício-Fernandes G, Laranjeira M (2000) Química Nova 23:441–446
13. Jungbauer A, Hahn R, Deinhofer K, Luo P (2004) Biotechnol Bioeng 87:364–374
14. Hsu F, Tsai S, Lan C, Wang Y (2005) J Mater Sci: Mater Med 16:341–345
15. Zhang R, Ma PX (1999) J Biomed Mater Res 285–293
16. Bigi A, Boanini E, Gazzano M, Rubini K (2005) Cryst Res Technol 40:1094–1098
17. Malkaj P, Pierri E, Dalas E (2005) J Mater Sci: Mater Med 16:733–737
18. Montemegro RVD, PhD thesis (2003) Crystallization, biomimetics and semiconducting polymers in confined systems. Golm, Germany
19. Kong L, Gao Y, Cao W, Gong Y, Zhao N, Zhang X (2005) J Biomed Mater Res A 75:275–282
20. Wan ACA, Khor E, Hastings GW (1997) J Biomed Mater Res 38:235–241
21. Boduch-Lee KA, Chapman T, Petricca SE, Marra KG, Kumta P (2004) Macromolecules 37:8959–8966
22. Chen H, Holl MB, Orr BG, Majoros I, Clarkson BH (2003) J Dent Res 82:443–448
23. Kaneko T, Ogomi D, Mitsugi R, Serizawa T, Akashi M (2004) Chem Mater 16:5596–5601
24. Song J, Saiz E, Bertozzi CR (2003) J Am Chem Soc 125:1236–1243
25. Song J, Malathong V, Bertozzi CR (2005) J Am Chem Soc 127:3366–3372
26. Tamai H, Yasuda H (1999) J Colloid Interface Sci 212:585–588
27. Schukin DG, Sukhorukov GB, Möhwald H (2003) Angew Chem (Int Ed) 42:4472–4475
28. Pich A, Bhattacharya S, Adler H-JP (2005) Polymer 46:1077–1086
29. Agarwal M, Pich A, Pionteck J, Ziferopolus N, Simon F, Stamm M (2007) Chem Mater 19:1845–1852
30. Pich A, Hain J, Prots Y, Adler H-JP (2005) Polymer 46:7931–7944
31. Agarwal R, Bell JP (1998) Polym Eng Sci 38:299–310
32. Bertolin M, Zecca M, Favero G, Palma G, Lora S, Ajo D, Corain B (1997) J Appl Polym Sci 65:2201–2207
33. Pich A, Wage T, Taubenberger A, Bhattacharya S, van Pee K-H, Adler H-J, (2006) Macromol Biosci 6:301–310